Analysis of a finite element method for the Stokes–Poisson–Boltzmann equations

Abeer F. AlSohaim[1] Ricardo Ruiz-Baier[2]
Segundo Villa-Fuentes[3]

(Received 9 February 2025; revised 6 August 2025)

Abstract

We define a finite element method for the coupling of Stokes and nonlinear Poisson–Boltzmann equations. The novelty in the formulation is that the coupling from the electric potential to the drag in the momentum balance is rewritten as a weighted advection term. Using Banach's contraction principle, the Babuška–Brezzi theory, and the Minty–Browder theorem, we show that the governing equations have a unique weak solution. We also show that the discrete problem is well-posed, establish Céa estimates, and derive convergence rates. We exemplify the properties of the proposed scheme via some numerical experiments showcasing convergence and applicability in the study of electro-osmotic flows in micro-channels.

DOI:10.21914/anziamproc.v66.19580, Published 2025-10-28, as part of the Proceedings of the 21st Biennial Computational Techniques and Applications Conference. ISSN 1445-8810.

Contents

1 Introduction

Scope. Electrically charged flows are of utmost importance in chemistry applications that concern, for example, the design of nanopores for biomedical devices and the modelling of water purification systems. One of the simplest processes to transport fluid without mechanical stimulation is electro-osmosis. In electro-osmosis, the mobility of electrolytic fluid is due to thin double layers that attract and repel ions, and it can be described by the Stokes equations with a forcing term that depends on the charge of the electrolyte and an externally applied electric field. In a simplified scenario, the flow itself, or its pressure gradients, are not dominant enough to influence the distribution of the double layer electrostatic potential, and so the electric charge density can be simply related to the potential using (even simplified versions of) the Poisson–Boltzmann equation.

Regarding unique solvability and finite element (FE) discretisation for the Poisson–Boltzmann equation we refer to Chen et al. [7] [also, e.g., 9, 10, 11] who use a splitting between regular and singular contribution expansions, apply convex minimisation arguments, and show an L^∞ bound for the solution using a cutoff-function approach. Here we take the regularised counterpart of the Poisson–Boltzmann equation, which maintains the same type of nonlinearity (a hyperbolic sine) but does not include the distributional Dirac forcing terms. In addition, here we also include an advection term in the regularised potential equation, and following Holst et al. [9] we restrict the functional space of the double layer potential to a bounded set (in turn, permitting us to have a bounded nonlinear operator).

Outline. The remainder of this section presents the strong form of the coupled system. Section 2 is devoted to the weak formulation and well-posedness using Banach fixed-point theory. In Section 3 we show the existence and uniqueness of a discrete solution, and outline the a priori error analysis. Finally, in Section 4 we provide numerical examples of convergence and fully developed electro-osmotic flows in eccentric micro-tubes.

The Stokes–Poisson–Boltzmann equations. Let us consider a Lipschitz bounded domain in $\mathbb{R}^n$, $n = 2, 3$ with boundary $\partial\Omega = \Gamma_D \cup \Gamma_N$ split into two parts where different types of boundary conditions are considered, and denote by $\mathbf{n}$ the outward unit normal vector on the boundary. The domain is filled with an incompressible electrolytic fluid subjected to pressure gradients and electric fields. The set of equations that govern the stationary regime are written in terms of fluid velocity $\mathbf{u}$, pressure p, and electrostatic double layer potential ψ, and are

$$-\mu\Delta\mathbf{u} + \nabla p = \mathbf{f} - \varepsilon\Delta\psi\mathbf{E} \qquad \text{in } \Omega\,, \tag{1a}$$
$$\operatorname{div}\mathbf{u} = 0 \qquad \text{in } \Omega\,, \tag{1b}$$
$$\kappa(\psi) + \mathbf{u}\cdot\nabla\psi - \varepsilon\Delta\psi = g \qquad \text{in } \Omega\,, \tag{1c}$$
$$\mathbf{u} = \mathbf{0} \quad \text{and} \quad \psi = 0 \qquad \text{on } \Gamma_D\,, \tag{1d}$$
$$(\mu\boldsymbol{\nabla}\mathbf{u} - p\mathbf{I})\mathbf{n} = \mathbf{0} \quad \text{and} \quad \varepsilon\nabla\psi\cdot\mathbf{n} = 0 \qquad \text{on } \Gamma_N\,. \tag{1e}$$

Here $\mathbf{I}$ is the identity tensor in $\mathbb{R}^{n\times n}$, μ is the fluid viscosity, $\mathbf{f} \in \mathbf{L}^2(\Omega)$ is a vector of external body forces, $\mathbf{E} \in \mathbf{L}^\infty(\Omega)$ is an externally applied electric field (typically along the longitudinal direction, and assumed uniformly bounded by $\bar{E} > 0$), ε is the electric permittivity of the electrolyte, $g \in L^2(\Omega)$ is an external source/sink of potential, and $\kappa(\psi) = k_0 \sinh(k_1\psi)$ is the charge of the electrolyte as a nonlinear function of potential, where $k_0 > 0$ depends on the valence, the electron charge, and the bulk ion concentration, and $k_1 > 0$

depends additionally on the Boltzmann constant and the reference absolute temperature. Following Holst et al. [9, Lem. 2.1] we assume that

- the potential is uniformly bounded between the values $\alpha \le 0 \le \beta \in \mathbb{R}$.

In addition, we assume $\kappa(0) = 0$, and that there exists $\bar{K}, \underline{K} > 0$ such that

- $|\kappa(s_1) - \kappa(s_2)| \le \bar{K}|s_1 - s_2|$ for all $s_1, s_2 \in [\alpha, \beta]$,
- $|\kappa(s_1) - \kappa(s_2)| \ge \underline{K}|s_1 - s_2|$ for all $s_1, s_2 \in [\alpha, \beta]$.

Homogeneity of (1d)–(1e) simplifies the exposition; however, the results remain valid for more general assumptions.

2 Existence and uniqueness of weak solution

Weak formulation. Consider the test and trial functional spaces for velocity, double layer potential, and pressure, respectively:

$$\begin{aligned} &\mathbf{V} := \{\boldsymbol{v} \in \mathbf{H}^1(\Omega) : \boldsymbol{v} = \mathbf{0} \text{ on } \Gamma_D\}, \quad \Phi_0 := \{\varphi \in H^1(\Omega) : \varphi = 0 \text{ on } \Gamma_D\}, \\ &\Phi := \{\varphi \in H^1(\Omega) : \varphi = 0 \text{ on } \Gamma_D \text{ and } \alpha \le \varphi \le \beta\}, \quad Q := L^2(\Omega). \end{aligned}$$

Then, multiplying (1a)–(1c) by suitable test functions, integrating by parts, and employing the boundary conditions, we are left with the weak formulation: find $(\mathbf{u}, p, \psi) \in \mathbf{V} \times Q \times \Phi$ such that

$$a(\mathbf{u}, \boldsymbol{v}) + A^{\psi}(\mathbf{u}, \boldsymbol{v}) + b(\boldsymbol{v}, p) = F^{\psi}(\boldsymbol{v}) \qquad \forall \boldsymbol{v} \in \mathbf{V}, \tag{2a}$$

$$b(\mathbf{u}, q) = 0 \qquad \forall q \in Q, \tag{2b}$$

$$(\kappa(\psi), \varphi) + c(\mathbf{u}; \psi, \varphi) + d(\psi, \varphi) = G(\varphi) \qquad \forall \varphi \in \Phi_0, \tag{2c}$$

where the bilinear and trilinear forms are

$$\begin{aligned} a(\mathbf{u}, \boldsymbol{v}) &:= \mu \int_\Omega \boldsymbol{\nabla} \mathbf{u} : \boldsymbol{\nabla} \boldsymbol{v}, \qquad & b(\boldsymbol{v}, q) &:= -\int_\Omega \operatorname{div} \boldsymbol{v}\, q, \\ c(\boldsymbol{v}; \psi, \varphi) &:= \int_\Omega (\boldsymbol{v} \cdot \nabla \psi)\varphi, \qquad & d(\psi, \varphi) &:= \varepsilon \int_\Omega \nabla \psi \cdot \nabla \varphi, \end{aligned}$$

and (for a fixed $\hat{\psi}$) the *linear* functionals and bilinear form are

$$F^{\hat{\psi}}(\boldsymbol{v}) := \int_\Omega \{\mathbf{f} + [g - \kappa(\hat{\psi})]\mathbf{E}\} \cdot \boldsymbol{v} \,,$$
$$G(\varphi) := \int_\Omega g\,\varphi \,, \quad A^{\hat{\psi}}(\boldsymbol{u}, \boldsymbol{v}) := \int_\Omega [\boldsymbol{u} \cdot \nabla\hat{\psi}](\mathbf{E} \cdot \boldsymbol{v}) \,.$$

Note that the specific forms of $F^{\psi}(\cdot)$ and $A^{\psi}(\cdot\,,\,\cdot)$ do not have the electric permittivity ε, since the weak formulation we propose comes from rewriting the last source term on the right-hand side of (1a) using the potential equation (1c). This has the advantage that the term containing the Laplacian of the potential in the momentum equation does not need to integrated by parts, and it gives us a more convenient structure for the fixed-point analysis.

The previously presented bilinear and trilinear forms are uniformly bounded. That is, for all $\boldsymbol{u}$, $\boldsymbol{v} \in \mathbf{V}$, $q \in Q$, ψ, $\hat{\psi} \in \Phi$ and $\varphi \in \Phi_0$,

$$|a(\boldsymbol{u}, \boldsymbol{v})| \le \mu\|\boldsymbol{u}\|_{1,\Omega}\|\boldsymbol{v}\|_{1,\Omega} \,, \quad |b(\boldsymbol{v}, q)| \le \|\boldsymbol{v}\|_{1,\Omega}\|q\|_{0,\Omega} \,,$$
$$|d(\psi, \varphi)| \le \varepsilon\|\psi\|_{1,\Omega}\|\varphi\|_{1,\Omega} \,, \quad |c(\boldsymbol{v}; \psi, \varphi)| \le C_{\mathrm{Sob}}^2\|\boldsymbol{v}\|_{1,\Omega}\|\psi\|_{1,\Omega}\|\varphi\|_{1,\Omega} \,,$$
$$|A^{\hat{\psi}}(\boldsymbol{u}, \boldsymbol{v})| \le C_{\mathrm{Sob}}^2\bar{E}\|\hat{\psi}\|_{1,\Omega}\|\boldsymbol{u}\|_{1,\Omega}\|\boldsymbol{v}\|_{1,\Omega} \,.$$

Their proof comes from Hölder's inequality and the estimate $\|\phi\|_{L^4(\Omega)} \le C_{\mathrm{Sob}}\|\phi\|_{1,\Omega}$, and is valid for all $\phi \in H^1(\Omega)$ [c.f., 13, Th. 1.3.3]. Similarly, the linear functionals in $\mathbf{V}'$ and Φ' are uniformly bounded (under the assumption that $\hat{\psi}$ is in a bounded set):

$$|F^{\hat{\psi}}(\boldsymbol{v})| \le \left[\|\mathbf{f}\|_{0,\Omega} + \bar{E}\|g\|_{0,\Omega} + \bar{K}\bar{E}\|\hat{\psi}\|_{1,\Omega}\right]\|\boldsymbol{v}\|_{1,\Omega} \,, \quad |G(\varphi)| \le \|g\|_{0,\Omega}\|\varphi\|_{1,\Omega} \,.$$

Using the Poincaré inequality $\|\phi\|_{1,\Omega} \le C_p|\phi|_{1,\Omega}$, with $C_p > 0$ and valid for all $\phi \in \{\varphi \in H^1(\Omega) : \varphi = 0 \text{ on } \Gamma_D\}$, it is not difficult to see that the bilinear forms $a(\cdot\,,\,\cdot)$ and $d(\cdot\,,\,\cdot)$ are coercive in $\mathbf{V}$ and Φ, respectively:

$$|a(\boldsymbol{v}, \boldsymbol{v})| \ge \mu[C_p^2]^{-1}\|\boldsymbol{v}\|_{1,\Omega}^2 \quad \forall \boldsymbol{v} \in \mathbf{V} \,,$$
$$|d(\varphi, \varphi)| \ge \varepsilon[C_p^2]^{-1}\|\varphi\|_{1,\Omega}^2 \quad \forall \varphi \in \Phi_0 \,.$$

Furthermore, $b(\cdot\,,\,\cdot)$ satisfies the inf-sup condition [e.g. 8]

$$\sup_{\boldsymbol{v}\in\mathbf{V}\setminus\{\mathbf{0}\}} \frac{b(\boldsymbol{v},q)}{\|\boldsymbol{v}\|_{1,\Omega}} \geq \beta\,\|q\|_{0,\Omega} \quad \forall q \in Q\,.$$

Well-posedness analysis. We employ a fixed-point argument in combination with the Babuška–Brezzi theory [4] and the Minty–Browder theorem [5]. The analysis closely follows the approach by Álvarez et al. [2] and Caucao et al. [6] for Boussinesq-type problems, where one separates the incompressible flow equations from the nonlinear transport equation and then connects them back using Banach's fixed-point theorem. First, consider the set

$$Z := \left\{\hat{\psi} \in \Phi : \quad \|\hat{\psi}\|_{1,\Omega} \leq \mu[2C_p^2 C_{\mathrm{Sob}}^2 \bar{E}]^{-1}\right\}, \tag{3}$$

and, for a fixed $\hat{\psi} \in Z$; the problem of finding $(\boldsymbol{u}, p) \in \mathbf{V} \times Q$ such that

$$\begin{aligned} a(\boldsymbol{u},\boldsymbol{v}) + A^{\hat{\psi}}(\boldsymbol{u},\boldsymbol{v}) + b(\boldsymbol{v},p) &= F^{\hat{\psi}}(\boldsymbol{v}) \quad \forall \boldsymbol{v} \in \mathbf{V}\,, \\ b(\boldsymbol{u},q) &= 0 \quad \forall q \in Q\,. \end{aligned} \tag{4}$$

We recall that the Stokes equations with mixed boundary conditions are uniquely solvable [8]. This is a consequence of the properties of $[a + A^{\hat{\psi}}](\cdot\,,\,\cdot)$:

$$\begin{aligned} |a(\boldsymbol{u},\boldsymbol{v}) + A^{\hat{\psi}}(\boldsymbol{u},\boldsymbol{v})| &\leq \left(\mu + \mu[2C_p^2]^{-1}\right) \|\boldsymbol{u}\|_{1,\Omega}\|\boldsymbol{v}\|_{1,\Omega}\,, \\ |a(\boldsymbol{v},\boldsymbol{v}) + A^{\hat{\psi}}(\boldsymbol{v},\boldsymbol{v})| &\geq \mu[2C_p^2]^{-1}\|\boldsymbol{v}\|_{1,\Omega}^2\,, \end{aligned} \tag{5}$$

which arise from the properties of $a(\cdot\,,\,\cdot)$ and $A^{\hat{\psi}}(\cdot\,,\,\cdot)$, the definition of Z, and the continuity and stability of $b(\cdot\,,\,\cdot)$. We therefore conclude that the operator

$$\mathcal{S}^{\mathrm{flow}} : \Phi \to \mathbf{V} \times Q\,, \quad \hat{\psi} \mapsto \mathcal{S}^{\mathrm{flow}}(\hat{\psi}) = (\mathcal{S}_1^{\mathrm{flow}}(\hat{\psi}), \mathcal{S}_2^{\mathrm{flow}}(\hat{\psi})) := (\boldsymbol{u}, p)\,,$$

is well-defined. Moreover, the continuous dependence on data ($\mathbf{f}, g$ and $\hat{\psi}$) provided by the Babuška–Brezzi theory [4] gives, in particular, that

$$\|\boldsymbol{u}\|_{1,\Omega} \leq 2C_p^2\mu^{-1}\left(\|\mathbf{f}\|_{0,\Omega} + \bar{E}\|g\|_{0,\Omega} + \bar{K}\bar{E}\|\hat{\psi}\|_{1,\Omega}\right). \tag{6}$$

Associated with the velocity, we define the set

$$\mathbf{W} := \left\{ \hat{\mathbf{u}} \in \mathbf{V} : \|\hat{\mathbf{u}}\|_{1,\Omega} \le \varepsilon[2C_{\mathrm{p}}^2 C_{\mathrm{Sob}}^2]^{-1} \right\}, \tag{7}$$

and consider, for a fixed $\hat{\mathbf{u}} \in \mathbf{W}$, the problem of finding $\psi \in \Phi$ such that

$$(\kappa(\psi), \varphi) + c(\hat{\mathbf{u}}; \psi, \varphi) + d(\psi, \varphi) = G(\varphi) \quad \forall \varphi \in \Phi_0 . \tag{8}$$

Using Hölder and Cauchy–Schwarz inequalities we proceed to verify that the operator associated with this problem is bounded:

$$|(\kappa(\psi), \varphi) + c(\hat{\mathbf{u}}; \psi, \varphi) + d(\psi, \varphi)| \le (\bar{K} + \varepsilon + C_{\mathrm{Sob}}^2 \|\hat{\mathbf{u}}\|_{1,\Omega}) \, \|\psi\|_{1,\Omega} \|\varphi\|_{1,\Omega} .$$

Next we use the coercivity of $d(\cdot\,,\,\cdot)$, the definition of $\mathbf{W}$, and the monotonicity of $\kappa(\cdot)$, to obtain the strong monotonicity of the solution operator

$$\begin{aligned}(\kappa(\psi_1) - \kappa(\psi_2), \psi_1 - \psi_2) + c(\hat{\mathbf{u}}\,; \psi_1 - \psi_2, \psi_1 - \psi_2) + d(\psi_1 - \psi_2, \psi_1 - \psi_2) \\ \ge \varepsilon[2C_{\mathrm{p}}^2]^{-1} \|\psi_1 - \psi_2\|_{1,\Omega}^2 \quad \forall\, \psi_1, \psi_2 \in \Phi .\end{aligned} \tag{9}$$

Then, the Minty–Browder theorem gives that there exists a unique $\psi \in \Phi$ so the map

$$\mathcal{S}^{\mathrm{elec}} : \mathbf{V} \to \Phi , \quad \hat{\mathbf{u}} \mapsto \mathcal{S}^{\mathrm{elec}}(\hat{\mathbf{u}}) = \psi ,$$

is well-defined. In addition, using (9), we have that the solution satisfies

$$\|\psi\|_{1,\Omega} \le 2C_{\mathrm{p}}^2 \varepsilon^{-1} \|g\|_{0,\Omega} . \tag{10}$$

Then, we introduce an operator equivalent to the solution map of (2):

$$\mathbf{T} : \mathbf{W} \to \mathbf{W} , \quad \hat{\mathbf{u}} \mapsto \mathbf{T}(\hat{\mathbf{u}}) := \mathcal{S}_1^{\mathrm{flow}}(\mathcal{S}^{\mathrm{elec}}(\hat{\mathbf{u}})) . \tag{11}$$

Lemma 1. *Assume that $\mathbf{f} \in \mathbf{L}^2(\Omega)$ and $g \in L^2(\Omega)$ satisfy the small data condition*

$$4C_{\mathrm{p}}^4 C_{\mathrm{Sob}}^2 [\mu\varepsilon]^{-1} \left(1 + \bar{E} + 2\bar{K}\bar{E}C_{\mathrm{p}}^2 \varepsilon^{-1}\right) (\|\mathbf{f}\|_{0,\Omega} + \|g\|_{0,\Omega}) \le 1 . \tag{12}$$

Then, the operator $\mathbf{T}$ is well-defined and $\mathbf{T}(\mathbf{W}) \subseteq \mathbf{W}$.

Proof: Given $\hat{\mathbf{u}} \in \boldsymbol{W}$, (12) implies $\frac{4C_p^4 C_{\text{Sob}}^2 \bar{E}}{\mu\varepsilon}\|g\|_{0,\Omega} \le 1$. Combining this with (10) gives $\mathcal{S}^{\text{elec}}(\hat{\mathbf{u}}) \in Z$. Since $\mathcal{S}^{\text{elec}}$ and $\mathcal{S}^{\text{flow}}$ are well-defined, it follows that $\mathbf{T}$ is well-defined. Moreover, from (6) and (10), we obtain

$$\|\mathcal{S}_1^{\text{flow}}(\mathcal{S}^{\text{elec}}(\hat{\mathbf{u}}))\|_{1,\Omega} \le 2C_p^2\mu^{-1}\left(\|\mathbf{f}\|_{0,\Omega} + \bar{E}\|g\|_{0,\Omega} + \bar{K}\bar{E}2C_p^2\varepsilon^{-1}\|g\|_{0,\Omega}\right).$$

Combining this with the small data assumption (12), we conclude that $\mathbf{T}(\hat{\mathbf{u}}) \in \boldsymbol{W}$, thereby completing the proof. ♠

Theorem 2. *Assume that* (12) *holds, and assume that*

$$4C_p^4 C_{Sob}^2 \bar{E}[\mu\varepsilon^2]^{-1}(\varepsilon + 2C_p^2\bar{K})\|g\|_{0,\Omega} < 1. \tag{13}$$

Then, $\mathbf{T}$ *has a unique fixed point* $\mathbf{u} \in \boldsymbol{W}$. *Equivalently, problem* (2) *has a unique solution* $(\mathbf{u}, p, \psi) \in \mathbf{V} \times Q \times \Phi$ *with* $\mathbf{u} \in \boldsymbol{W}$. *Moreover,*

$$\|\psi\|_{1,\Omega} \lesssim \|g\|_{0,\Omega} \quad \textit{and} \quad \|\mathbf{u}\|_{1,\Omega} + \|p\|_{0,\Omega} \lesssim \|\mathbf{f}\|_{0,\Omega} + \|g\|_{0,\Omega}. \tag{14}$$

Proof: Given $\hat{\mathbf{u}}_1, \hat{\mathbf{u}}_2 \in \boldsymbol{W}$, we let $\psi_1, \psi_2 \in \Phi_0$ such that $\mathcal{S}^{\text{elec}}(\hat{\mathbf{u}}_1) = \psi_1$ and $\mathcal{S}^{\text{elec}}(\hat{\mathbf{u}}_2) = \psi_2$. Using (8), adding $\pm c(\hat{\mathbf{u}}_1, \psi_2, \varphi)$, taking $\varphi = \psi_1 - \psi_2$, and applying (9) along with the boundedness of $c(\cdot;\cdot,\cdot)$, we obtain

$$\|\mathcal{S}^{\text{elec}}(\hat{\mathbf{u}}_1) - \mathcal{S}^{\text{elec}}(\hat{\mathbf{u}}_2)\|_{1,\Omega} \le 2C_{\text{Sob}}^2 C_p^2 \varepsilon^{-1}\|\psi_2\|_{1,\Omega}\|\hat{\mathbf{u}}_1 - \hat{\mathbf{u}}_2\|_{1,\Omega}. \tag{15}$$

Similarly, let $\hat{\psi}_1, \hat{\psi}_2 \in \Phi$ and $(\mathbf{u}_1, p_1), (\mathbf{u}_2, p_2) \in \mathbf{V}\times Q$, such that $\mathcal{S}^{\text{flow}}(\hat{\psi}_1) = (\mathbf{u}_1, p_1)$ and $\mathcal{S}^{\text{flow}}(\hat{\psi}_2) = (\mathbf{u}_2, p_2)$. Using (4), adding $\pm A^{\hat{\psi}_1}(\mathbf{u}_2, \boldsymbol{v})$, taking $\boldsymbol{v} = \mathbf{u}_1 - \mathbf{u}_2$, and applying the coercivity of $a + A^{\hat{\psi}}(\cdot\,,\cdot)$ (c.f. (5)), along with the continuity of $A^{\hat{\psi}}(\cdot\,,\cdot)$ and the assumptions for $\kappa(\cdot)$, we have

$$\|\mathcal{S}_1^{\text{flow}}(\hat{\psi}_1) - \mathcal{S}_1^{\text{flow}}(\hat{\psi}_2)\|_{1,\Omega} \le 2C_p^2\bar{E}\mu^{-1}(C_{\text{Sob}}^2\|\mathbf{u}_2\|_{1,\Omega} + \bar{K})\|\hat{\psi}_1 - \hat{\psi}_2\|_{1,\Omega}. \tag{16}$$

Thus, combining (15) with (16), we have

$$\|\mathbf{T}(\hat{\mathbf{u}}_1) - \mathbf{T}(\hat{\mathbf{u}}_2)\|_{1,\Omega} \le \|\mathcal{S}_1^{\text{flow}}(\mathcal{S}^{\text{elec}}(\hat{\mathbf{u}}_1)) - \mathcal{S}_1^{\text{flow}}(\mathcal{S}^{\text{elec}}(\hat{\mathbf{u}}_2))\|_{1,\Omega}$$

$$\leq 2C_p^2\bar{E}\mu^{-1}(C_{\text{Sob}}^2\|\mathbf{u}_2\|_{1,\Omega}+\bar{K})2C_{\text{Sob}}^2C_p^2\varepsilon^{-1}\|\mathcal{S}^{\text{elec}}(\hat{\mathbf{u}}_2)\|_{1,\Omega}\|\hat{\mathbf{u}}_1-\hat{\mathbf{u}}_2\|_{1,\Omega}\,.$$

Then, using the fact that $\mathcal{S}^{\text{elec}}(\hat{\mathbf{u}}_2)$ satisfies (10) and that $\hat{\mathbf{u}}_2$ (and therefore, thanks to Lemma 1, also $\mathbf{u}_2$) is in $\boldsymbol{W}$, we obtain

$$\|\mathbf{T}(\hat{\mathbf{u}}_1)-\mathbf{T}(\hat{\mathbf{u}}_2)\|_{1,\Omega}\leq 8C_p^6C_{\text{Sob}}^2\bar{E}[\mu\varepsilon^2]^{-1}\left(\varepsilon[2C_p^2]^{-1}+\bar{K}\right)\|g\|_{0,\Omega}\|\hat{\mathbf{u}}_1-\hat{\mathbf{u}}_2\|_{1,\Omega}\,,$$

which together with (13) and the Banach fixed-point theorem implies that $\mathbf{T}$ has a unique fixed point in $\boldsymbol{W}$. Finally, the first estimate in (14) is derived similarly to (10), while the second follows directly from Ern and Guermond [8, Th. 2.34]. ♠

3 Finite element discretisation

Define $\mathcal{T}_h$ as a shape-regular simplicial mesh of Ω with mesh-size $h := \max\{h_K : K \in \mathcal{T}_h\}$. Given $k \geq 1$, the generalised Taylor–Hood FE spaces for the approximation of velocity, pressure, and potential, are

$$\begin{aligned}
\mathbf{V}_h &:= \{\boldsymbol{v}_h \in \mathbf{C}^0(\Omega) : \boldsymbol{v}_h|_K \in [\mathbb{P}_{k+1}(K)]^n\,,\ \forall K \in \mathcal{T}_h\,,\ \boldsymbol{v}_h = \mathbf{0} \text{ on } \Gamma_D\}\,,\\
Q_h &:= \{q_h \in C^0(\Omega) : q_h|_K \in \mathbb{P}_k(K)\,, K \in \mathcal{T}_h\}\,,\\
\Phi_h &:= \{\varphi_h \in C^0(\Omega) : \varphi_h|_K \in \mathbb{P}_{k+1}(K)\,,\ \forall K \in \mathcal{T}_h\,, \varphi_h = 0 \text{ on } \Gamma_D\}\,.
\end{aligned}$$

The FE scheme then reads: find $(\mathbf{u}_h, p_h, \psi_h) \in \mathbf{V}_h \times Q_h \times \Phi_h$ such that

$$a(\mathbf{u}_h,\boldsymbol{v}_h)+A^{\psi_h}(\mathbf{u}_h,\boldsymbol{v}_h)+b(\boldsymbol{v}_h,p_h)=F^{\psi_h}(\boldsymbol{v}_h)\qquad\forall\boldsymbol{v}_h\in\mathbf{V}_h\,,\tag{17a}$$

$$b(\mathbf{u}_h,q_h)=0\qquad\forall q_h\in Q_h\,,\tag{17b}$$

$$(\kappa(\psi_h),\varphi_h)+c(\mathbf{u}_h;\psi_h,\varphi_h)+d(\psi_h,\varphi_h)=G(\varphi_h)\qquad\forall\varphi_h\in\Phi_h\,.\tag{17c}$$

The unique solvability of the discrete problem can be shown using similar techniques as for the continuous counterpart.

Theorem 3. *Suppose that the assumptions of Theorem 2 hold. Then, (17) has a unique solution $(\mathbf{u}_h, p_h, \psi_h) \in \mathbf{V}_h \times Q_h \times \Phi_h$. Moreover,*

$$\|\psi\|_{1,\Omega}\lesssim\|g\|_{0,\Omega}\quad\textit{and}\quad\|\mathbf{u}\|_{1,\Omega}+\|p\|_{0,\Omega}\lesssim\|\mathbf{f}\|_{0,\Omega}+\|g\|_{0,\Omega}\,.\tag{18}$$

Theorem 4. *Let* $(\mathbf{u}, p, \psi), (\mathbf{u}_h, p_h, \psi_h)$ *be the continuous and discrete solutions. Then, assuming that the datum* g *satisfies*

$$\left(1 + 4\varepsilon^{-1}\bar{K}\bar{E}C_p^2\right) 4\varepsilon^{-1} C_{\mathrm{Sob}}^2 C_p^2 \|g\|_{0,\Omega} \leq 1\,, \tag{19}$$

we have a bound, with hidden constant independent of h*:*

$$\|\mathbf{u}-\mathbf{u}_h\|_{1,\Omega}+\|p-p_h\|_{0,\Omega}+\|\psi-\psi_h\|_{1,\Omega} \lesssim \operatorname{dist}(\mathbf{u}, \mathbf{V}_h)+\operatorname{dist}(p, Q_h)+\operatorname{dist}(\psi, \Phi_h)\,.$$

Proof: For a given $(\hat{\boldsymbol{v}}_h, \hat{q}_h, \hat{\varphi}_h) \in \mathbf{V}_h \times Q_h \times \Phi_h$, let us decompose errors using $\boldsymbol{\xi}_{\mathbf{u}} := \mathbf{u} - \hat{\boldsymbol{v}}_h$, $\boldsymbol{\chi}_{\mathbf{u}} := \hat{\boldsymbol{v}}_h - \mathbf{u}_h$, $\xi_p := p - \hat{q}_h$, $\chi_p := \hat{q}_h - p_h$, $\xi_\psi := \psi - \hat{\varphi}_h$ and $\chi_\psi := \hat{\varphi}_h - \psi_h$. Proceeding as in Theorem 2, we obtain

$$\begin{aligned}\|\boldsymbol{\chi}_{\mathbf{u}}\| + \|\chi_p\| + \|\chi_\psi\| \leq{}& \tfrac{4}{\varepsilon}\bar{K}\bar{E}C_{\mathrm{Sob}}^2 C_p^2 \|\psi_h\|_{1,\Omega}\|\mathbf{u}-\mathbf{u}_h\|_{1,\Omega} + \varepsilon\|\xi_\psi\|_{1,\Omega}\\ &+ C_{\mathrm{Sob}}^2\|\psi\|_{1,\Omega}\|\mathbf{u}-\mathbf{u}_h\|_{1,\Omega} + (1+\mu)\|\boldsymbol{\xi}_{\mathbf{u}}\|_{1,\Omega} + \|\xi_p\|_{0,\Omega}\\ &+ C_{\mathrm{Sob}}^2\|\mathbf{u}_h\|_{1,\Omega}\|\xi_\psi\|_{1,\Omega} + C_{\mathrm{Sob}}^2\bar{E}\|\psi_h\|_{1,\Omega}\|\boldsymbol{\xi}_{\mathbf{u}}\|_{1,\Omega}\,.\end{aligned}$$

♠

Finally, the following result is a direct consequence of Theorem 4 and standard interpolation properties for Taylor–Hood FEs [8].

Theorem 5. *Let* $(\mathbf{u}, p, \psi), (\mathbf{u}_h, p_h, \psi_h)$ *be the continuous and discrete solutions assuming* $\mathbf{u} \in \mathbf{V} \cap \mathbf{H}^{s+1}(\Omega)$, $p \in H^s(\Omega)$, *and* $\psi \in \Phi \cap H^{s+1}(\Omega)$, *for some* $s \in (1/2, k+1]$. *Then, there exists* $C > 0$, *independent of* h, *such that*

$$\|\mathbf{u}-\mathbf{u}_h\|_{1,\Omega}+\|p-p_h\|_{0,\Omega}+\|\psi-\psi_h\|_{1,\Omega} \leq C\,h^s\{\|\mathbf{u}\|_{1+s,\Omega}+|p|_{s,\Omega}+\|\psi\|_{1+s,\Omega}\}\,.$$

4 Numerical results

We now provide three simple computational tests confirming the convergence of the method and simulating electrically charged fluid in a container and a channel. They have been carried out with the library `Gridap` [3]. We use a Newton–Raphson method with a residual tolerance of 10^{-7}. In the first

Table 1: Convergence history. Errors, experimental rates, and Newton iteration count for FE families using polynomial degrees $k = 1, 2$.

DOF	h	$e(\mathbf{u})$	$r(\mathbf{u})$	$e(p)$	$r(p)$	$e(\psi)$	$r(\psi)$	it
				$k = 1$				
57	0.7071	6.50e-01	$\star$	2.21e-01	$\star$	2.65e-01	$\star$	4
217	0.3536	1.79e-01	1.860	3.49e-02	2.658	6.96e-02	1.927	4
849	0.1768	4.66e-02	1.943	6.97e-03	2.325	1.78e-02	1.969	4
3361	0.0884	1.18e-02	1.979	1.64e-03	2.089	4.48e-03	1.987	4
13377	0.0442	2.97e-03	1.992	4.04e-04	2.022	1.12e-03	1.995	4
53377	0.0221	7.45e-04	1.997	1.01e-04	2.006	2.82e-04	1.998	4
213249	0.0110	1.86e-04	1.998	2.51e-05	2.001	7.05e-05	1.999	4
				$k = 2$				
133	0.7071	1.38e-01	$\star$	3.01e-02	$\star$	3.39e-02	$\star$	4
513	0.3536	1.86e-02	2.899	4.12e-03	2.871	4.37e-03	2.955	4
2017	0.1768	2.35e-03	2.980	5.41e-04	2.926	5.51e-04	2.988	4
8001	0.0884	2.95e-04	2.995	6.87e-05	2.979	6.92e-05	2.995	4
31873	0.0442	3.69e-05	2.999	8.62e-06	2.995	8.66e-06	2.998	4
127233	0.0221	4.61e-06	2.999	1.08e-06	2.997	1.09e-06	2.994	4
508417	0.0110	5.80e-07	2.992	1.51e-07	2.939	1.63e-07	2.939	4

test, the convergence rates from Theorem 5 are studied using the unit square domain $\Omega = (0,1)^2$ and the manufactured solutions to (1):

$$\mathbf{u} := \begin{pmatrix} \cos(\pi x)\sin(\pi y) \\ -\sin(\pi x)\cos(\pi y) \end{pmatrix}, \quad p := \sin(\pi x)\sin(\pi y)\,, \quad \psi := \cos(\pi(x+y))\,.$$

The Dirichlet boundary corresponds to the bottom and right segments and the Neumann boundary to the top and left. The constants assume unity values $k_0 = k_1 = \mu = \varepsilon = 1$, $\mathbf{E} = (0,-1)^t$, and the forcing term and non-homogeneous boundary data are computed from the manufactured solutions. The error decay is reported in Table 1, where we also tabulate rates of convergence $r(\cdot) = \log(e_{(\cdot)}/\tilde{e}_{(\cdot)})[\log(h/\tilde{h})]^{-1}$, where $e, \tilde{e}$ denote errors generated on two consecutive meshes of sizes h and $\tilde{h}$, respectively. Optimal convergence is

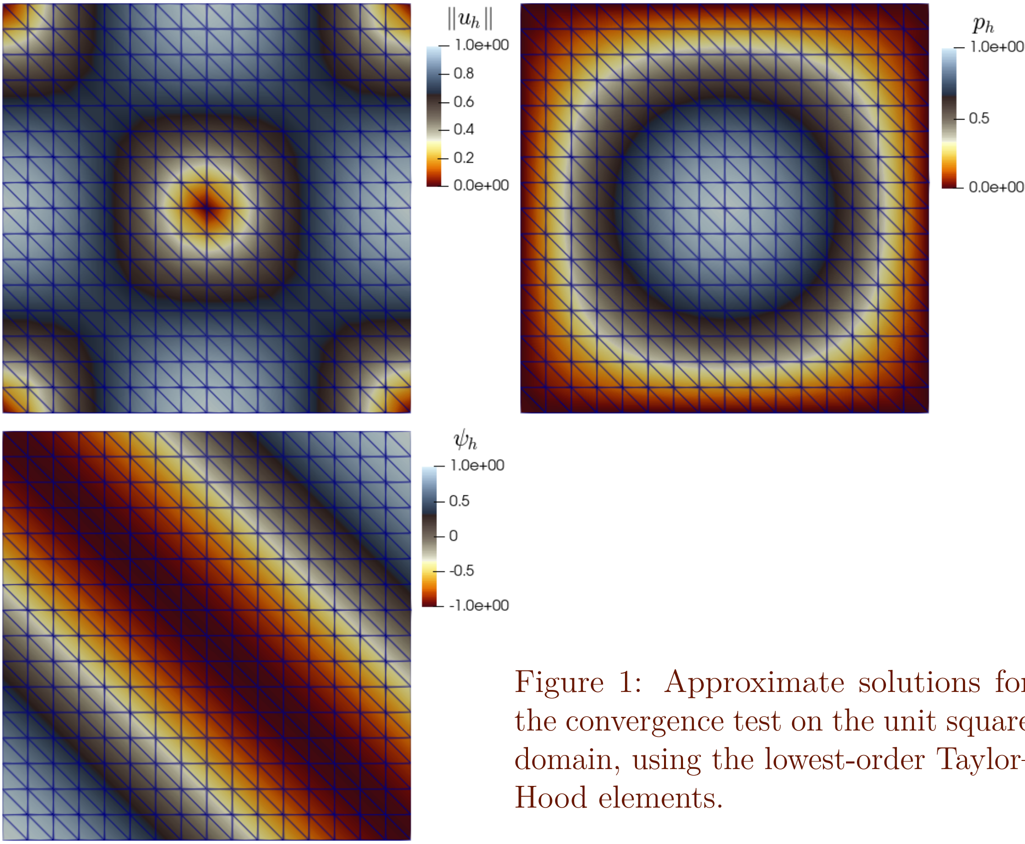

Figure 1: Approximate solutions for the convergence test on the unit square domain, using the lowest-order Taylor–Hood elements.

verified in all fields, and the approximate solutions plotted in Figure 1 show well-resolved profiles even for coarse meshes.

Next we study the electro-osmotic and pressure-driven mixing of a fluid in a micro-annulus following the configuration of Akyildiz et al. [1], but instead of bipolar coordinates we employ a full 3D Cartesian system. The model parameters are set to $\mu = 10^{-2}$, $r_1 = 1$, $r_2 = 2$, $H = 0.75$, $k_1 = 1$, $\mathbf{E} = (0, 0, 1)^t$, and

$$k_0 = \frac{(H - r_1 - r_2)(H - r_1 + r_2)(H + r_1 - r_2)(H + r_1 + r_2)}{2H} .$$

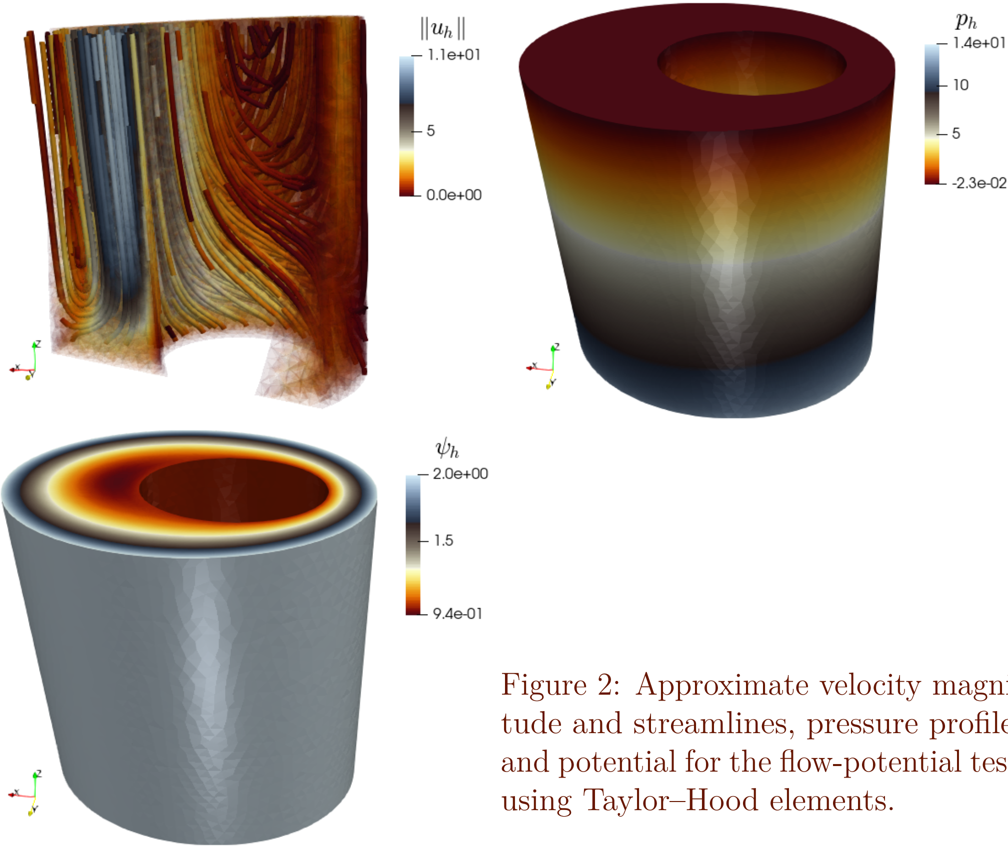

Figure 2: Approximate velocity magnitude and streamlines, pressure profile, and potential for the flow-potential test using Taylor–Hood elements.

On the outer annulus we impose $\psi = 2$, on the inner one we set $\psi = 1$ and leave zero-flux boundary conditions elsewhere. We set $\mathbf{u} = (0, 0, 1)^{\mathrm{t}}$ on the bottom face, no slip velocity on the inner and outer annulus $\mathbf{u} = \mathbf{0}$, and outflow conditions on the top face. For this test we discard advection (so that only the charge and inlet velocity determine the flow patterns). The results in Figure 2 show a higher electro-osmotic fluid mobility near the narrow part of the channel, and a distribution of the double layer potential comparable to the profiles obtained in Akyildiz et al. [1].

Finally, we present a simulation of electrically charged flow in a nanopore

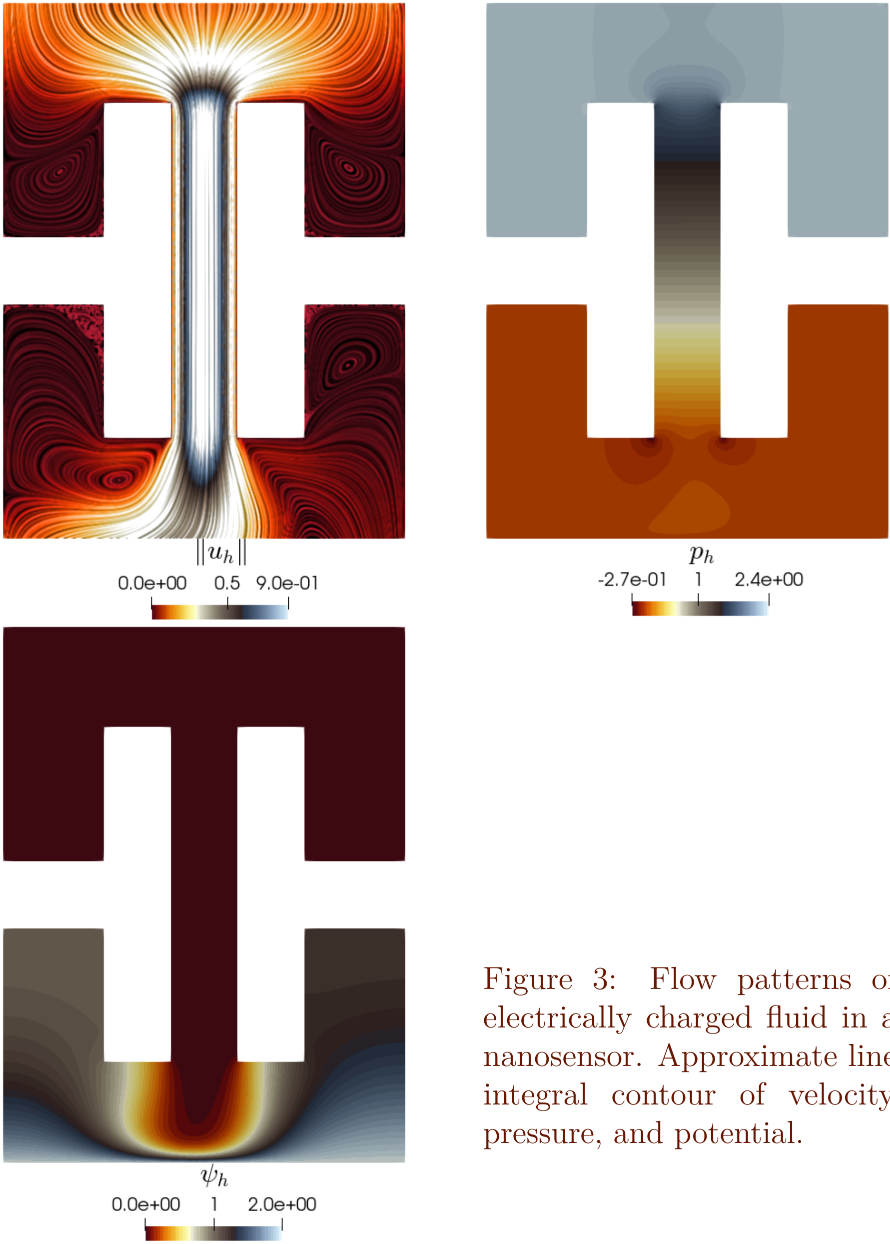

Figure 3: Flow patterns of electrically charged fluid in a nanosensor. Approximate line integral contour of velocity, pressure, and potential.

sensor with obstacles. The geometry of size $12\,\text{nm} \times 16\,\text{nm}$ and flow configuration are adapted from Mitscha-Baude et al. [12, Section 4.5] (although their work focuses on Poisson–Nernst–Planck/Stokes equations). An ionic current is generated by a difference of potential on the top and bottom of the nanopore $\psi_{\max} = 2$, $\psi_{\min} = 0$. Also, a parabolic inflow velocity $\boldsymbol{u}_{\text{in}} = (0, -0.1\tanh(40(6-x)^2))^t$ is imposed on the top boundary and outflow boundary conditions are applied on the bottom. On the outer left and right segments, we impose a slip condition ($\boldsymbol{u} \cdot \boldsymbol{n} = 0$) and on the remainder of the boundary we impose no-slip conditions for the velocity $\boldsymbol{u} = \boldsymbol{0}$ and zero-flux for the potential. For this example, we incorporate again the advective term in the potential equation as well as the convective nonlinearity in the momentum balance, and consider the following parameter values

$$\mu = 0.1\,\text{Pa}\cdot\text{s}, \quad \varepsilon = 0.075\,, \quad \boldsymbol{E} = (0.1, -0.1)^t\,, \quad k_0 = 10^{-3}\,.$$

The aim of the example is simply to simulate the electric patterns and corresponding flow associated with an applied field pointing not straight down, but with a slight angle to break symmetry. In Figure 3 we show the velocity line integral contours, the pressure drop and the potential distribution. Thanks to a comparable drag force used herein, we see recirculation similar to that of Mitscha-Baude et al. [12, Section 4.5]. For this test, the total number of degrees of freedom is $157\,676$, and the Newton–Raphson solver takes seven iterations to reach the prescribed tolerance.

Acknowledgements. This research was supported by the Australian Research Council through the Future Fellowship FT220100496 and Discovery Project DP22010316; and by the National Research and Development Agency (ANID) of Chile through the postdoctoral grant Becas Chile 74220026.

References

[1] F. T. Akyildiz, A. F. A. AlSohaim, and N. Kaplan. "Electro-osmotic and pressure-driven flow in an eccentric microannulus". In: *Zeitschr.*

Nat. A 74.6 (2019), pp. 513–521. DOI: 10.1515/zna-2018-0483 (cit. on pp. C12, C13).

[2] M. Alvarez, G. N. Gatica, and R. Ruiz-Baier. “A mixed-primal finite element method for the coupling of Brinkman–Darcy flow and nonlinear transport”. In: *IMA J. Numer. Anal.* 41.1 (2021), pp. 381–411. DOI: 10.1093/imanum/drz060 (cit. on p. C6).

[3] S. Badia, A. F. Martín, and F. Verdugo. “GridapDistributed: A massively parallel finite element toolbox in Julia”. In: *J. Open Source Softw.* 7.74, 4157 (2022). DOI: 10.21105/joss.04157 (cit. on p. C10).

[4] D. Boffi, F. Brezzi, and M. Fortin. *Mixed Finite Element Methods and Applications*. Vol. 44. Berlin: Springer-Verlag, 2013. DOI: 10.1007/978-3-642-36519-5 (cit. on p. C6).

[5] Philippe G. C. *Linear and Nonlinear Functional Analysis with Applications*. Society for Industrial and Applied Mathematics: SIAM, 2013. DOI: 10.1137/1.9781611978247 (cit. on p. C6).

[6] S. Caucao, R. Oyarzúa, and S. Villa-Fuentes. “A new mixed-FEM for steady-state natural convection models allowing conservation of momentum and thermal energy”. In: *Calcolo* 57.4, 36 (2020). DOI: 10.1007/s10092-020-00385-3 (cit. on p. C6).

[7] L. Chen, M. J. Holst, and J. Xu. “The finite element approximation of the nonlinear Poisson–Boltzmann equation”. In: *SIAM J. Numer. Anal.* 45.6 (2007), pp. 2298–2320. DOI: 10.1137/060675514 (cit. on p. C2).

[8] A. Ern and J.-L. Guermond. *Theory and Practice of Finite Elements*. New York: Applied Mathematical Sciences, 159. Springer-Verlag, 2004. DOI: 10.1007/978-1-4757-4355-5 (cit. on pp. C6, C9, C10).

[9] M. Holst, J. A. McCammon, Z. Yu, Y. C. Zhou, and Y. Zhu. “Adaptive finite element modeling techniques for the Poisson–Boltzmann equation”. In: *Comm. Comput. Phys.* 11.1 (2012), 179–214. DOI: 10.4208/cicp.081009.130611a (cit. on pp. C2, C4).

[10] J. A. Iglesias and S. Nakov. “Weak formulations of the nonlinear Poisson-Boltzmann equation in biomolecular electrostatics”. In: *J. Math. Anal. Appl.* 511.1 (2022), p. 126065. DOI: 10.1016/j.jmaa.2022.126065 (cit. on p. C2).

[11] J. Kraus, S. Nakov, and S. I. Repin. “Reliable numerical solution of a class of nonlinear elliptic problems generated by the Poisson–Boltzmann equation”. In: *Comput. Methods Appl. Math.* 20.2 (2020), pp. 293–319. DOI: 10.1515/cmam-2018-0252 (cit. on p. C2).

[12] Gregor Mitscha-Baude, Andreas Buttinger-Kreuzhuber, Gerhard Tulzer, and Clemens Heitzinger. “Adaptive and iterative methods for simulations of nanopores with the PNP–Stokes equations”. In: *J. Comput. Phys.* 338 (2017), pp. 452–476. DOI: 10.1016/j.jcp.2017.02.072 (cit. on p. C15).

[13] A. Quarteroni and A. Valli. *Numerical Approximation of Partial Differential Equations*. Vol. 23. Springer Series in Computational Mathematics. Springer-Verlag, Berlin, 1994, pp. xvi+543. DOI: 10.1007/978-3-540-85268-1 (cit. on p. C5).

Author addresses

1. **Abeer F. AlSohaim**, School of Mathematics, Monash University, 9 Rainforest Walk, 3800 VIC, Australia; Department of Mathematics and Statistics, College of Science, IMSIU (Imam Mohammad Ibn Saud Islamic University), Riyadh, Saudi Arabia.
   mailto:abeer.alsohaim@monash.edu

2. **Ricardo Ruiz-Baier**, School of Mathematics, Monash University, 9 Rainforest Walk, 3800 VIC, Australia.
   mailto:ricardo.ruizbaier@monash.edu
   orcid:0000-0003-3144-5822

3. **Segundo Villa-Fuentes**, School of Mathematics, Monash University, 9 Rainforest Walk, 3800 VIC, Australia.

mailto:segundo.villafuentes@monash.edu
orcid:0000-0002-0377-6555